Resonance Stabilized Perfluorinated Ionomers for Alkaline Membrane Fuel Cells

ARTICLE *in* MACROMOLECULES · JANUARY 2013

Impact Factor: 5.8 · DOI: Doi 10.1021/Ma401568f

6 AUTHORS, INCLUDING:

Yoong-Kee Choe
National Institute of Advanced Industrial Scie…
36 PUBLICATIONS **686** CITATIONS
SEE PROFILE

Yu Seung Kim
Los Alamos National Laboratory
114 PUBLICATIONS **5,976** CITATIONS
SEE PROFILE

Macromolecules

Article

pubs.acs.org/Macromolecules

Resonance Stabilized Perfluorinated Ionomers for Alkaline Membrane Fuel Cells

Dae Sik Kim,[†,#] Cy H. Fujimoto,[‡] Michael R. Hibbs,[§] Andrea Labouriau,[⊥] Yoong-Kee Choe,[∥] and Yu Seung Kim*,[†]

[†]Sensors and Electrochemical Devices Group, Los Alamos National Laboratory, Los Alamos, New Mexico 87545, United States

[‡]Organic Materials Science, Sandia National Laboratory, Albuquerque, New Mexico 87185, United States

[§]Materials, Devices, & Energy Technologies Group, Sandia National Laboratory, Albuquerque, New Mexico 87185, United States

[⊥]Polymers and Coatings Group, Los Alamos National Laboratory, Los Alamos, New Mexico 87545, United States

[∥]National Insititute of Advanced Industrial Science & Technology, Tsukuba, 305-8575, Japan

Supporting Information

ABSTRACT: Perfluorosulfonic acids such as Nafion are industrial standard cation exchange ionomers for polymer electrolyte membrane fuel cells because of their high gas permeability, hydrophobicity, and inertness to electro-chemical reaction. In this research, pentamethylguanidinium functionalized, perfluorinated hydroxide conducting ionomers for alkaline membrane fuel cells were prepared and characterized. The alkaline stability of the ionomers largely depended on the adjacent group that connected the cation; Sulfone guanidinium functionalized ionomer degraded almost completely after soaking in 0.5 M NaOH at 80 °C for 24 h, while phenylguanidinium functionalized ionomer did not degrade under the same conditions for 72 h. Spectroscopic data and density functional theory calculation suggested that the stability of the phenylguanidinium ionomer was greatly improved by charge delocalization of the formed resonance structure. Alkaline membrane fuel cells using the resonance stabilized perfluorinated ionomer in the catalyst layers on quaternized polyphenylene membrane showed excellent performance (ca. maximum power density = 466 mW/cm^2) and promising stability (*ca. Tafel* slope degradation rate = 225 μV/dec h) at 80 °C under H_2/air conditions.

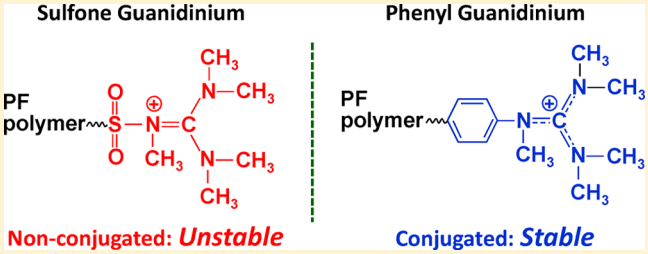

1. INTRODUCTION

One of the key advances in proton exchange membrane fuel cells (PEMFCs) was made by Ian Raistrick of Los Alamos National Laboratory (LANL), who began impregnating electrodes with perfluorinated ionomer in liquid dispersions.[1] This technique greatly reduced interfacial resistance, enabled lower catalyst loading, and improved fuel cell performance by an order of magnitude with respect to conventional PEMFC electrodes at that time. This technique was later refined by Mahlon Wilson of LANL[2] and is used today by all PEMFC manufacturers and researchers.

Alkaline membrane fuel cells (AMFCs) are currently drawing tremendous attention since nonprecious metal catalysts have shown good oxygen reduction reaction (ORR) activities under high pH environments.[3] However, current AMFC performances using nonprecious or even precious metal catalysts are inferior to its PEMFC counterpart.[4] For example, state-of-the-art PEMFC with Pt-based electrodes yield power density of >500 mW/cm^2 at 0.7 V under H_2/air conditions[4d] while analogous AMFC with higher Pt loading electrodes only yields power densities of <200 mW/cm^2 at 0.7 V under H_2/air (CO_2 free) conditions.[4e] Some of the performance lag of AMFCs can be related to the relatively low hydroxide mobility compared to proton mobility. However, the performance differences between the two systems cannot be explained solely by conductivity differences.

Another cause for the inferior performance is that typical AMFCs use hydrocarbon-based ionomers in the catalyst layer, while PEMFCs use perfluorinated ionomers. In previous studies, the benefits of using perfluorinated ionomer in the PEMFC catalyst layers have been described in various aspects:[5] (i) higher oxygen permeability; (ii) hydrophobicity; (iii) less anion absorption onto catalyst (ca. less catalyst poisoning); (iv) facile polymer chain mobility/relaxation; (v) ability to create a porous electrode structure. Although the perfluorinated ionomers in the catalyst layer have been recognized in PEMFCs, there is no such analogue for AMFCs. In addition, limited synthetic efforts have been made in this endeavor. Direct replacement of sulfonic acid groups of perfluorosulfonated polymer with hydroxide conducting cationic groups is difficult due to the instability of the fluoroalkylamine intermediate. Even successfully synthesized polymers of this

Received: July 25, 2013
Revised: September 4, 2013
Published: September 18, 2013

Scheme 1. Synthetic Procedure of (a) Sulfone−Pentamethylguanidinium and (b) Phenylpentamethylguanidinium Functionalized Perfluorinated Ionomers

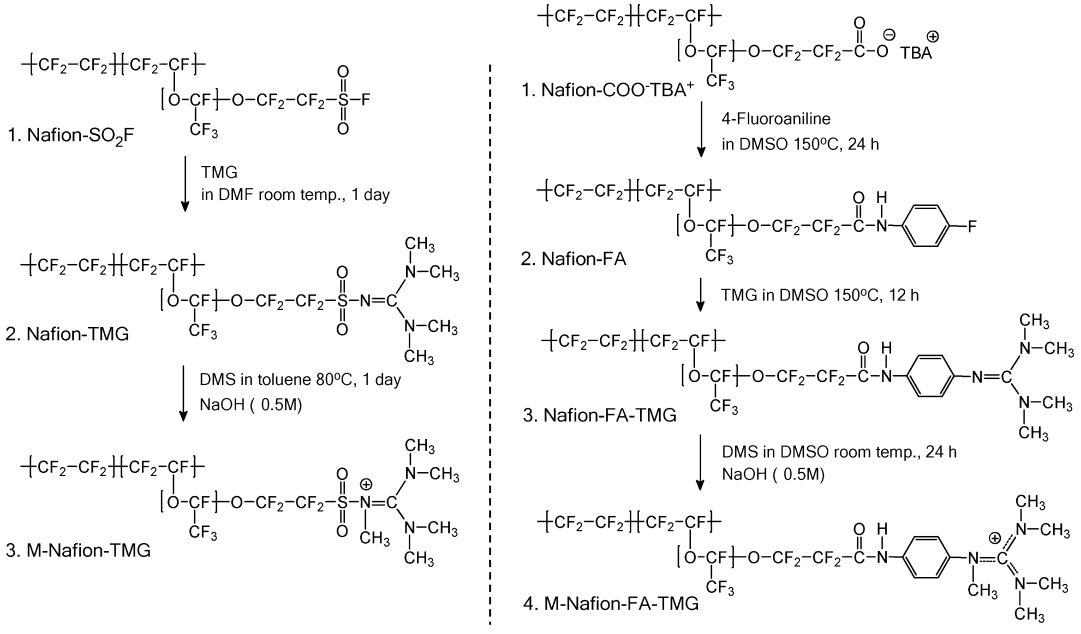

type (e.g., Tosflex) are not stable under high pH environments because of the strong electron withdrawing characteristic of perfluoroalkyls.[6] An alternative and easier method in preparing perfluorinated ionomers is through sulfone−cation bonds.[7] Unfortunately, these bonds are relatively weak and an "onium" salt may form as an intermediate that rapidly break down in water to liberate the amine.

Sluggish reaction kinetics with the alkyl ammonium hydroxide could be another reason for the inferior AMFC performance.[8] Unlu et al. reported that the anodic hydrogen desorption of Pt in quaternary ammonium hydroxide was 2.6 times slower than that in NaOH due to the specific adsorption of the cation.[8a] Interestingly, we found that the hydrogen evolution/oxidation reaction (HER/HOR) and ORR kinetics of Pt and carbon-based non precious metal catalysts could be significantly improved by replacing the ammonium hydroxide with guanidinium hydroxide.[8b−d] Although a comprehensive study of reaction kinetics with respect to cation type has not been pursued, results thus far suggest that the guanidinium hydroxide may be an attractive alternative to conventional ammonium hydroxide.

Herein, we report the synthesis and use of guanidinium-functionalized perfluorinated anion exchange ionomers as an electrode binder for AMFC. Guanidinium functionalization to polymer chains can be accomplished by several synthetic routes: (i) halomethylation of a phenyl group and subsequent amination with pentamethylguanidine;[9] (ii) nucleophilic substitution of a Vilsmeier salt and a secondary amine;[10] (iii) activated fluoroamine reaction.[11] The halomethylation/amination results in a benzylguanidinium and the reaction with the Vilsmeier salt and a secondary amine produces an alkylguanidinium. The activated fluoroamine reaction can form either a phenylguanidinium or sulfone−guanidinium. In this study, we used the activated fluoroamine reaction since (i) the sulfonyl fluoride form of Nafion precursor can be directly converted through amination and (ii) similarly the fluorophenyl can be aminated with tetramethylguanidine albeit at higher reaction temperatures. The alkaline stability of the ionomers prepared from the fluoroamine reaction is compared after immersion the materials in dilute NaOH and is examined with spectroscopy and quantum mechanical calculations. Finally, the performance and stability of AMFCs using the guanidinium functionalized perfluorinated ionomer are demonstrated.

2. EXPERIMENTAL SECTION

2.1. Materials. Nafion sulfonyl fluoride precursor (Nafion-SO_2F) and carboxylic acid form Nafion (Nafion-COOH) were purchased from Ion Power, Inc. Dimethylformamide (DMF) and dimethyl sulfoxide (DMSO) were purchased from Sigma-Aldrich and vacuum distilled prior to use. All other chemicals such as 1,1,3,3-tetramethylguanidine (TMG), 4-fluoroaniline (FA), tetrabutylammonium hydroxide (TBAOH), dimethyl sulfate (DMS), toluene, *N*-methylpyrrolidone (NMP), and glycerol were reagent grade from Acros Organics and were used as received.

2.2. Polymer Synthesis. Scheme 1 displays the synthetic schemes of sulfone−pentamethylguanidinium and phenylpentamethylguanidinium functionalized perfluorinated ionomers (M-Nafion-TMG and M-Nafion-FA-TMG, respectively). The synthesis of M-Nafion-TMG was accomplished with a two-step procedure: (i) attachment of TMG to Nafion-SO_2F via activated sulfone fluoride−amine reaction under anhydrous conditions and (ii) methylation with DMS at 80 °C. The synthesis of M-Nafion-FA-TMG was accomplished with a three-step procedure: (i) attachment of a FA spacer to Nafion-COOH, (ii) functionalization of TMG via activated phenyl fluoride-amine reaction, and (iii) methylation with DMS at room temperature. The perfluorocarboxylic acid was first converted to a tetrabutylammonium (TBA^+) salt by immersion in 12.5% TBAOH solution in order to increase solubility of the material in DMSO. Nafion-COO^-TBA^+ could be completely dissolved when heated to 130 °C. To this solution, 50 mol % excess of FA was added at 150 °C and reacted for 24 h to prepare Nafion-FA. The sulfate form membrane after methylation with DMS was cast from NMP or NMP/glycerol mixed solvents, which we used for the characterization after converting to the hydroxide form.

dx.doi.org/10.1021/ma401568f | *Macromolecules* 2013, 46, 7826−7833

2.3. Ionomer Characterization. The FT-IR spectra of the membranes were measured using a Nicolet IR 8700 spectrometer (Thermo Nicolet, Madison, WI), with spectra recorded at 4 cm^{-1} resolution and measuring 4000−700 cm^{-1}.

Solid-state NMR was carried out using a 400 Bruker Avance spectrometer operating at 100.6221 MHz for ^{13}C. MAS spectra were obtained by direct detection, samples were spun at 10 kHz and recycle time was 20 s. High-resolution ^{1}H NMR experiments were carried out using a Bruker Avance NMR spectrometer operating at 300.131 MHz for ^{1}H. Chemical shift for nuclei was referenced to internal methyl sulfoxide-d_6 (99.9 atom % D) (2.50 ppm for ^{1}H).

Hydroxide conductivities of the membranes were estimated from AC impedance spectroscopy using a Solartron 1260 gain phase analyzer over a frequency range from 1 Hz to 1 MHz. The sulfate form perfluorinated ionomers were first converted to the hydroxide from by immersion in 0.5 M NaOH solution for 1 h at room temperature, followed by washing with water at 80 °C several times. The anion conductivity (σ) in OH^- rich environments was measured in water degassed with N_2 gas to remove CO_2.[11] Sample strips had a dimension of approximately 0.5 × 1 in. and was seated between two Pt coated electrodes. The conductivity of the samples in the longitudinal direction was calculated, using the relationship $\sigma = L/(R \times d \times W)$ where L is the distance between the electrodes, d and W are the thickness and width of the sample strip, respectively. R was derived from the low intersect of the high frequency semicircle on a complex impedance plane with the Re(Z) axis.

Water uptake (WU) was calculated by setting the weight difference between the dry and wet membranes. The dried membranes were weighed and then soaked in water until the weight remained constant. The percent water uptake of membranes was calculated by the following equation: $WU = (W_{wet} - W_{dry})/W_{dry} \times 100$, where W_{wet} and W_{dry} the weight of the wet and dry membranes, respectively.

2.4. Density Functional Theory Calculation. Density functional theory (DFT) calculations were performed using the Gaussian 09 suite of programs.[12] Geometry optimization and harmonic vibrational frequency calculations were performed employing wB97xD functional developed by Head-Gordon et al.[13] with 6-311++G(2d, 2p) basis set.[14] Effects of solvent water molecules were taken into consideration by the polarizable continuum model (PCM),[15] which is the default solvent reaction field calculation method in Gaussian 09. The vibrational frequency calculations were undertaken to check the nature of transition states and the presence of a single imaginary frequency and we observed one imaginary frequency associated with reaction coordinates.

2.5. Membrane Electrode Assembly and Fuel Cell Testing. For the fabrication of membrane electrode assembly (MEA), benzyltrimethyl ammonium functionalized poly(phenylene) (ATM-PP)[16] (thickness =50 μm) were used for the anion exchange membrane. High loading Pt black catalyst (HiSPEC 1000, Johnson Matthey) was used on both anode (3.4 mg_{Pt}/cm^2) and cathode (6.5 mg_{Pt}/cm^2) to minimize catalyst-related performance losses. Double-sided hydrophobic carbon cloths (ELAT, E-TEK Inc.) were used as electrode gas diffusion layers. Catalyst ink was prepared by mixing Pt black catalyst with sulfate form perfluorinated ionomer dispersion in NMP/glycerol 1:1 mixture (solid content: 1.5 wt %). The catalyst inks were painted on the membrane's surface and dried *in vacuo* for 2 h at 60 °C and further dried at 75 °C for 2 h. The MEAs were immersed into 0.5 M NaOH for 1 h, followed by washing with DI water at 80 °C several times.

The performance of MEAs was evaluated using 5 cm^2 single cell hardware (Fuel Cell Technologies Inc.). Initial polarization curves were obtained after a 15 h break-in at 80 °C under fully humidified conditions (90 and 80 °C dew point for anode and cathode, respectively, reactant backpressure at 30 psig). Pure H_2 and O_2 or house air (CO_2 content =10 ppm) were supplied to anode and cathode, respectively. An extended-term AMFC performance was evaluated under constant voltage of 0.6 V at 80 °C under fully humidified conditions. After the 11 and 120 h continuous operation, polarization curves and high frequency resistance (HFR) were obtained. The *i*R-free cell voltage, $E_{iR\text{-Free}}$ was determined by online HFR measurement. The reproducibility of AMFC performance using M-Nafion-FA-TMG was confirmed by testing at least three different batches.

3. RESULTS AND DISCUSSION

3.1. Synthesis of Sulfone−Guanidinium Functionalized Perfluorinated Ionomer (M-Nafion-TMG). M-Nafion-TMG was synthesized by nucleophilic substitution of the sulfonyl fluoride Nafion precursor with TMG and subsequent methylation. The sulfonyl fluoride−amine reaction proceeded easily without side reactions under anhydrous conditions. Under aqueous environments, however, hydrolysis of the sulfonyl fluoride occurred in preference to produce a perfluorosulfonated guanidinium salt ($CF_2SO_3^-TMG^+$), instead of perfluorosulfone−guanidine (CF_2SO_2-TMG). Figure 1

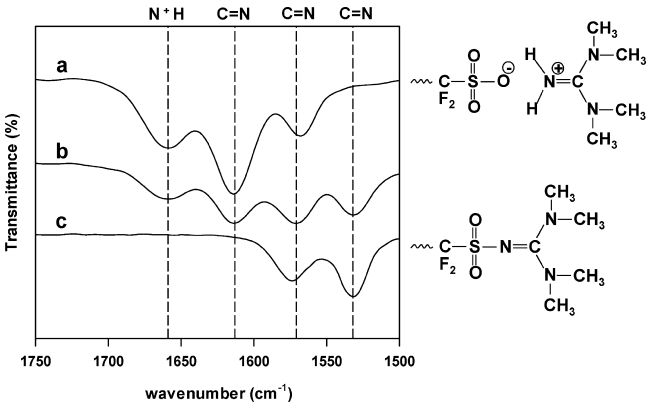

Figure 1. FT-IR spectra of Nafion-TMG from the reaction in (a) water, (b) commercial DMF, and (c) anhydrous DMF.

shows the FT-IR spectra of Nafion-TMG produced from water, commercial DMF and anhydrous DMF. Nafion-TMG from water exhibited an intense protonated C═N peak at 1615 cm^{-1} and a peak at 1568 cm^{-1}. Moreover, an intense peak at 1660 cm^{-1} is assigned to the protonated primary amine (i.e., N^+H) due to proton transfer from sulfonic acid to the NH group of TMG.[17] This result indicates that the sulfonyl fluoride-amine reaction in water produces the perfluorosulfonated guanidinium salt which is easily converted to the acid form by immersion in diluted sulfuric acid solution. Under anhydrous conditions, reaction between sulfonyl fluoride and guanidine did not produce the N^+H peak. Instead we observed the intense C═N peak at a substantially lower frequency (1533 cm^{-1}) while the other C═N peak was shifted slightly to a higher frequency (1574 cm^{-1}), indicating a deprotonated guanidine structure.[18] Nafion-TMG from a commercial DMF without distillation (water content: 0.15 wt %) exhibited all four characteristic peaks found under both water and anhydrous conditions, indicating that the resultant material was a mixture of perfluorosulfonated guanidinium and neutral perfluorosulfone-guanidine.

Methylation is a nucleophilic substitution reaction and the reaction efficiency depends on the leaving group of methylating agent. Methyl iodide is widely used for alkylating carbon, oxygen, sulfur and nitrogen nucleophiles. However the yield for methylation of Nafion-TMG using methyl iodide was less than 10%. Methyl iodide was then replaced by the more reactive DMS. Using this approach, the methylation yield approached 100% (Figure 2). M-Nafion-TMG exhibited an intense methylated C═N stretching peak at 1662 cm^{-1} (shifted from

dx.doi.org/10.1021/ma401568f | *Macromolecules* 2013, 46, 7826−7833

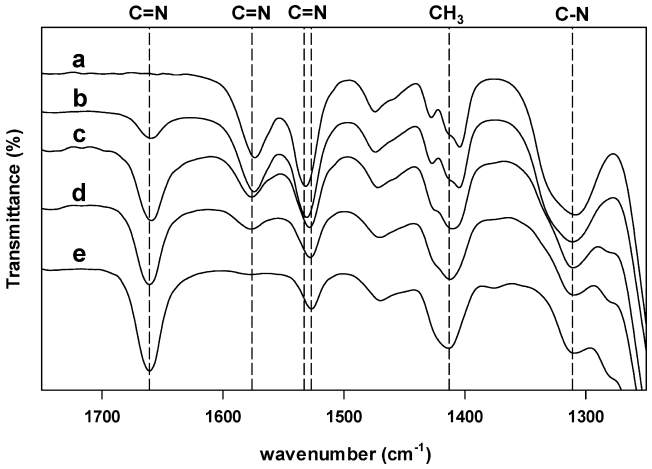

Figure 2. FT-IR spectra of Nafion-TMG during methylation using DMS: (a) before methylation; (b) 3 h; (c) 7 h; (d) 0 h; (e) 24 h.

1533 cm^{-1}) and a methylated C═N peak at 1527 cm^{-1} (shifted from 1574 cm^{-1}). Significant downshift of the C═N peak indicates that the guanidine structure converted to the guanidinium. The CH_3 peak at around 1414 cm^{-1} became broader, yet the position of the C−N peak of the guanidinium at 1310 cm^{-1} remained the same with reduced intensity.

Figure 3 shows the solid state ^{13}C NMR spectra of Nafion-TMG and M-Nafion-TMG. The central and methyl carbon

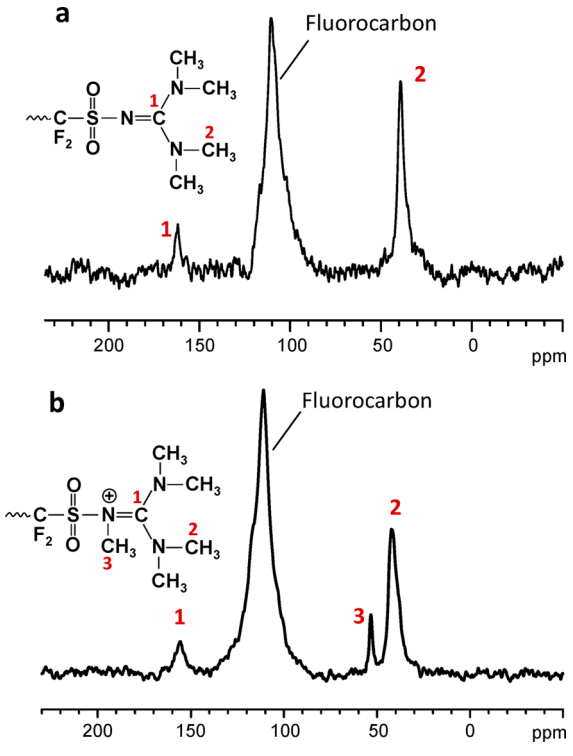

Figure 3. Solid state ^{13}C NMR spectra of (a) Nafion-TMG and (b) M-Nafion-TMG.

peaks of TMG before methylation appeared at 162 and 40 ppm, respectively. After methylation, the central carbon peak shifted to 156 ppm and the methyl carbon peak slightly shifted to 41 ppm. The upfield chemical shift of the central carbon indicates relatively high electron density. This result suggests that the sulfonyl nitrogen (not the central carbon) is positively charged. A new carbon peak of methyl group appeared at 52 ppm derived from methylation. The yield of methylation calculated from the integration ratio of C to (50−55 ppm, 3C) to C (28−50 ppm, 2C) was 98%.

3.2. Synthesis of Phenylguanidinium Functionalized Perfluorinated Ionomer (M-Nafion-FA-TMG). M-Nafion-FA-TMG was prepared from the direct amide coupling reaction between Nafion COO^-TBA^+ and FA in DMSO and subsequent phenyl fluoride-amine reaction, followed by methylation. No noticeable hydrolysis was observed during the phenyl fluoride-amine reaction. The methylation was performed using DMS under mild conditions. Figure 4 shows

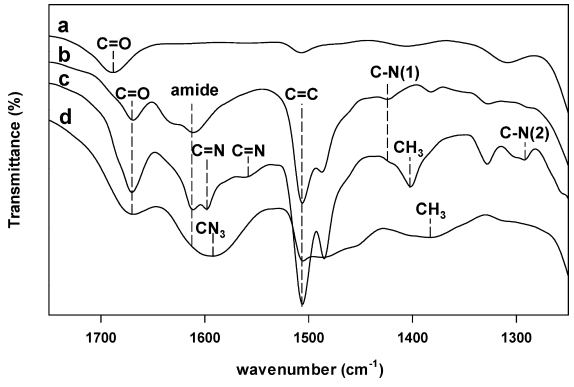

Figure 4. FT-IR spectra of (a) Nafion-COO^-TBA^+; (b) Nafion-FA; (c) Nafion-FA-TMG; (d) M-Nafion-FA-TMG.

FT-IR spectra during each synthetic step. The C═O peak of Nafion-COO^-TBA^+ at 1688 cm^{-1} shifted to a lower wavenumber (1669 cm^{-1}) after the reaction with Nafion-COO^-TBA^+ and FA, suggesting a conjugation of the carbonyl group. The new peaks of Nafion-FA are shown at 1611−1631 cm^{-1} (amide), 1487−1506 cm^{-1} (aromatic C═C), 1424 cm^{-1} (C−N (1) of amide). The new peaks derived from reaction between Nafion-FA and TMG appeared at 1558 and 1597 cm^{-1} (C═N of TMG), 1402 cm^{-1} (CH_3 of TMG), and 1292 cm^{-1} (C−N (2) of TMG) in Nafion-FA-TMG.[19] After methylation, a broad and single C═N stretching peak appeared at 1592 cm^{-1} and the intensity of C−N (2) of TMG reduced. The relatively low wavenumber of the methylated C═N double bond stretching peak compared to the methylated C═N peak observed with sulfone guanidinium (1662 cm^{-1}, Figure 2e) indicated a reduction of the amount of double bond character of phenylguanidinium. The weakened and broad nature of C═N (and CH_3) peak further supports the charge delocalization by forming a resonance structure.[20] Therefore, the imine peak should be described as CN_3 stretch, where the three CN bonds should be approximately identical. It was noted that the position of CN_3 peak is lower than the intense imine peaks of sulfonated guanidinium (1615 cm^{-1}, Figure 1a) and even 1,1,3,3 tetramethylguanidinium (1596 cm^{-1}, Figure S1, Supporting Information) which suggests that the charge delocalization of the guanidinium was enhanced by replacing the primary amine to tertiary (phenyl) amine.

Figure 5 shows the solid state ^{13}C NMR spectra of Nafion-FA-TMG and M-Nafion-FA-TMG. The central and methyl carbon peaks of TMG of Nafion-FA-TMG appeared at 158 and 39 ppm, respectively. After methylation, the central and methyl peaks slightly shifted to 159 and 38 ppm, respectively. The downfield peak shift of the central carbon suggests that the

dx.doi.org/10.1021/ma401568f | Macromolecules 2013, 46, 7826−7833

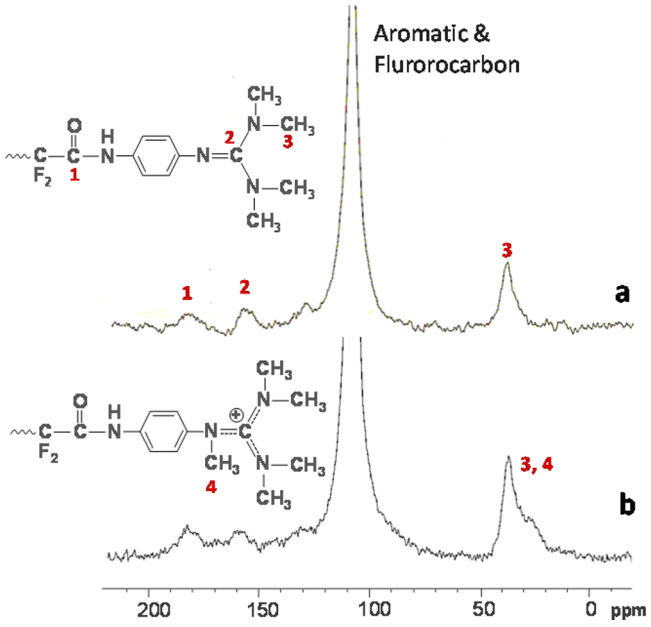

Figure 5. Solid state ^{13}C NMR spectra of (a) Nafion-FA-TMG and (b) M-Nafion-FA-TMG.

central carbon was positively charged by the formation of resonance structure, which is stark contrast with M-Nafion-TMG where a nonconjugated structure with positively charged nitrogen was formed. A new carbon peak appeared as a shoulder to the methyl peak of guanidinium at 27 ppm. Compared to the methyl peak of M-Nafion-TMG (52 ppm, 3C), the substantial upfield chemical shift indicates that the electron density of the phenylguanidinium greatly increased in the methyl group due to the electron donating phenyl group. The lower frequency of the added methyl group compared to the existed methyl groups of the phenylguanidinium suggests that the phenyl nitrogen has slightly higher electron density than the other amine groups. The TMG attachment yield calculated from the integration ratio of C (175−195 ppm, −C═O, 1C) to C (30−50 ppm, −TMG, 4C) was 95%. The chemical structure of the synthesized M-Nafion-FA-TMG was confirmed by ^{1}H NMR (Figure S2, Supporting Information). Chemical shifts of the amide group and the central carbon of guanidinium were observed at 4.25 and 3.15 ppm, respectively.[21] The chemical shift at 2.88 ppm is attributed to the methyl group from the methylation reaction. The yield of TMG attachment calculated from the integration ratio of protons of amide group (4.25 ppm, 1H), guanidinium (3.1−3.2 ppm −TMG, 12H), and methyl group (2.8−2.9 ppm, 3H) was nearly 100%, which was consistent with the ^{13}C NMR result.

3.3. Properties and Stability of the Perfluorinated Ionomers. Table 1 shows the electrochemical properties of the hydroxide form of the perfluorinated ionomers. The ion exchange capacity (IEC) of the polymers was calculated from the ^{1}H integral ratio (see example in Figure S2, Supporting Information). The IEC of M-Nafion-TMG was close to the targeted IEC (calculated from the equivalent weight of the Nafion precursor) and the IEC of M-Nafion-FA-TMG was 7% less than the targeted IEC. M-Nafion-TMG exhibited higher hydroxide conductivity and water uptake than M-Nafion-FA-TMG probably due to the IEC differences. When compared against hydrocarbon-based anion exchange ionomers, the perfluorinated ionomers have significantly higher hydroxide conductivity at a given IEC. For example, a poly(phenylene) ionomer with an IEC of 1.4 mequiv/g, exhibited hydroxide conductivity of 40 mS/cm at 80 °C.[16] The relatively higher conductivity of perfluorinated ionomers is because the higher density of fluorine atom (compared to hydrogen atom) shorten the ion conduction pathway at a given weight based IEC and enhance the conductivity.[22]

Table 1. IEC, Hydroxide Conductivity (σ) and Water Uptake (WU) of Perfluorinated Ionomers

	IEC (mequiv/g)		σ (mS/cm)		WU (wt %)
ionomer	target	expt	30 °C	80 °C	30 °C
M-Nafion-TMG	0.82	0.81	25	50	15
M-Nafion-FA-TMG	0.75	0.70	9	20	10

The alkaline stability of M-Nafion-TMG and M-Nafion-FA-TMG was compared. Figure 6 shows the FT-IR spectra of the perfluorinated ionomers before and after immersion in 0.5 M NaOH solution at 80 °C. For M-Nafion-TMG, the methylated C═N stretching peaks at 1662 and 1527 cm^{-1} disappeared and the trace of the CH_3 peak was shifted to 1373 cm^{-1} after 24 h NaOH treatment (Figure 6a). The ^{13}C NMR confirmed the structural change: the central carbon peak (156 ppm) almost disappeared and the peak from the carbon of the methyl group (40 ppm) was shifted to 30 ppm with a substantial loss of intensity (Figure S3, Supporting Information). The chemical shift of the methyl groups indicated that the electron density of the methyl group increased probably by the hydrolysis of sulfonyl or guanidinium group that liberated the cation from the polymer. In contrast, the CN_3 resonance and CH_3 peaks of M-Nafion-FA-TMG, remained unchanged after 72 h, under 0.5 M NaOH at 80 °C, indicating that the phenylguanidinium was stable (Figure 6b). The slight loss of intensity for the CN_3 resonance peak (~8%) accompanied by the peak intensity loss of the C═O stretching bend at 1660 cm^{-1} indicates possible hydrolysis of the amide group of M-Nafion-FA-TMG.

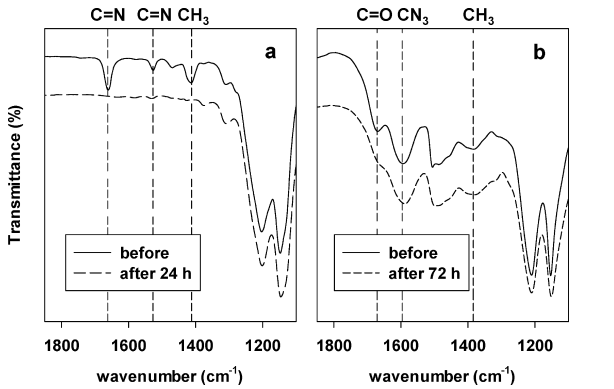

Figure 6. FT-IR spectra of (a) M-Nafion-TMG and (b) M-Nafion-FA-TMG before and after 0.5 M NaOH treatment at 80 °C.

We theoretically analyzed degradation reaction pathways of the guanidinium cations due to the attack of hydroxide ion. Figure 7 shows the energy profiles on the degradation of sulfone−pentamethylguanidinium and phenylpentamethylguanidinium. For sulfone−pentamethylguanidinium, the hydrolysis of sulfone group occurs in a barrierless manner. The central carbon of the sulfone−guanidinium with respect to the attack of hydroxide ion has slightly higher barrier energy (i.e., 2.0

dx.doi.org/10.1021/ma401568f | Macromolecules 2013, 46, 7826−7833

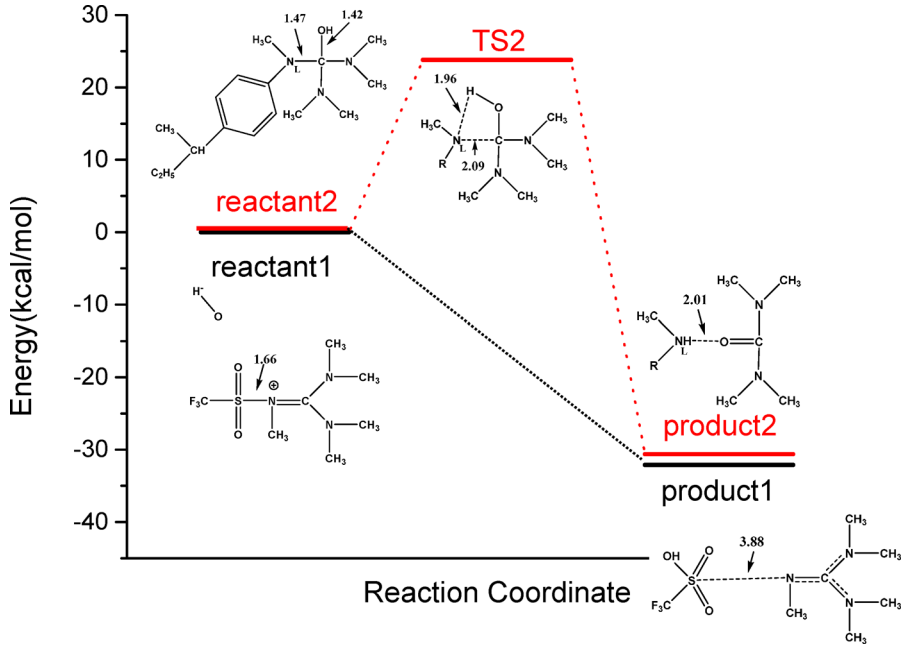

Figure 7. Energy profiles of the guanidinium degradation caused by OH^-; the redline corresponds to the profile for phenyl pentamethylguanidinium. Also, molecular structures of stationary points along the reaction coordinate are shown. Some geometrical parameters [distances in Å] are listed.

kcal/mol) than that of sulfone group hydrolysis (Figure S4, Supporting Information). On the other hand, the central carbon of the phenylguanidinium has much higher barrier energy (i.e., 23.8 kcal/mol). During the degradation of phenylguanidinium, hydroxide ion is attached to the central carbon of phenylguanidinium, then further degradation reactions proceeds from this complex.[23] The transition structure of phenylguanidnium degradation shows that the hydrogen atom is located close to N_L ("L" represents "leaving") while the bond between N_L and the central carbon is elongated. Finally, a urea is formed as a final product of the degradation. This modeling study indicates that the hydrolysis of sulfonic group occurs prior to the central carbon degradation of the guanidinium while the central carbon degradation of the phenylguanidinium occurs to produce tetramethyl urea with much higher barrier energy. Similar central carbon degradation of guanidinium has been proposed with 1,1,3,3-tetramethylguanidinium,[18a] yet we did not observe the degradation of phenylguanidinium in our experiments, possibly because of relatively short experimental time or more stable guanidinium structure (phenyl pentamethyl vs tetramethylguanidinium). Those computational results support the experimental observations.

3.4. AMFC Performance and Stability using the M-Nafion-FA-TMG Ionomer. The AMFC performance and durability using M-Nafion-FA-TMG as an ionomeric binder in the AMFC electrodes was investigated. Benzyl trimethylammonium functionalized poly(phenylene) (ATM-PP)[16] (thickness = 50 μm) was used as the anion exchange membrane separator. Figure 8**a** shows that the polarization curves of MEA using M-Nafion-FA-TMG at 80 °C. The MEA using M-Nafion-FA-TMG showed a maximum power density = 466 mW/cm^2 under H_2/air (CO_2 level in air: 10 ppm) and 577 mW/cm^2 under H_2/O_2 conditions. Considering that the state-of-the-art AMFC performance using thinner membranes exhibited the maximum power density of 250−300 mW/cm^2 under 50 °C, H_2/air (CO_2 free) conditions (Tokuyama Corporation) or 500 mW/cm^2 under 80 °C, H_2/O_2 conditions (CellEra),[24] the performance of the MEA using M-Nafion-FA-TMG was excellent. In order to investigate the possible reason for the performance improvement, we prepared a MEA having the same MEA components yet using benzyl trimethylammonium functionalized poly(phenylene) (ATM-PP)[16b] as an ionomeric binder. The MEA using ATM-PP exhibited substantially lower AMFC performance (ca. maximum power density =335 mW/cm^2 under H_2/O_2 conditions). It was also noted that the HFR of the MEA using the perfluorinated ionomer, particularly under H_2/O_2 conditions, was lower than the MEAs using ATM-PP, suggesting that the anion exchange membrane in the MEA was hydrated better through the hydrophobic perfluorinated ionomer-bonded electrode without interfacial failure[25] between the ATM-PP membrane and M-Nafion-FA-TMG-bonded electrodes. The improved AMFC performance using M-Nafion-FA-TMG in spite of the lower hydroxide conductivity (ca. 20 mS cm^{-1} for M-Nafion-FA-TMG vs 120 mS cm^{-1} for ATM-PP) suggests that (i) hydroxide conductivity of ionomer may have only a marginal impact on AMFC electrode performance and (ii) guanidinium cations and perfluorinated polymer backbone structure may render desirable three phase boundaries for the electrochemical reaction. Further electrochemical analysis including HOR and ORR kinetics, gas diffusion and relaxation behavior of the perfluorinated and hydrocarbon ionomer-bonded electrodes will be reported in a subsequent paper. Figure 8b shows the stability of the MEA using M-Nafion-FA-TMG was evaluated under H_2/air AMFC operation by monitoring the kinetic change of the *Tafel-slope* (ca. < 0.04 A cm^{-2}) of *iR*-corrected polarization curves with an assumption that the degradation of high loading-Pt black catalyst is negligible. The *Tafel-slope* of AMFC using M-Nafion-FA-TMG in the catalyst layers showed decay rate of 225 μV dec^{-1} h^{-1} during 80 °C, H_2/air AMFC operation. Considering the MEA using highly stable benzyl trimethylammonium functionalized ATM-PP exhibited the *Tafel-slope* change of 183 μV/dec h during 60 °C, H_2/O_2 AMFC operation,[16b] the ability of M-Nafion-FA-TMG to exhibit a similar decay rate at

dx.doi.org/10.1021/ma401568f | *Macromolecules* 2013, 46, 7826−7833

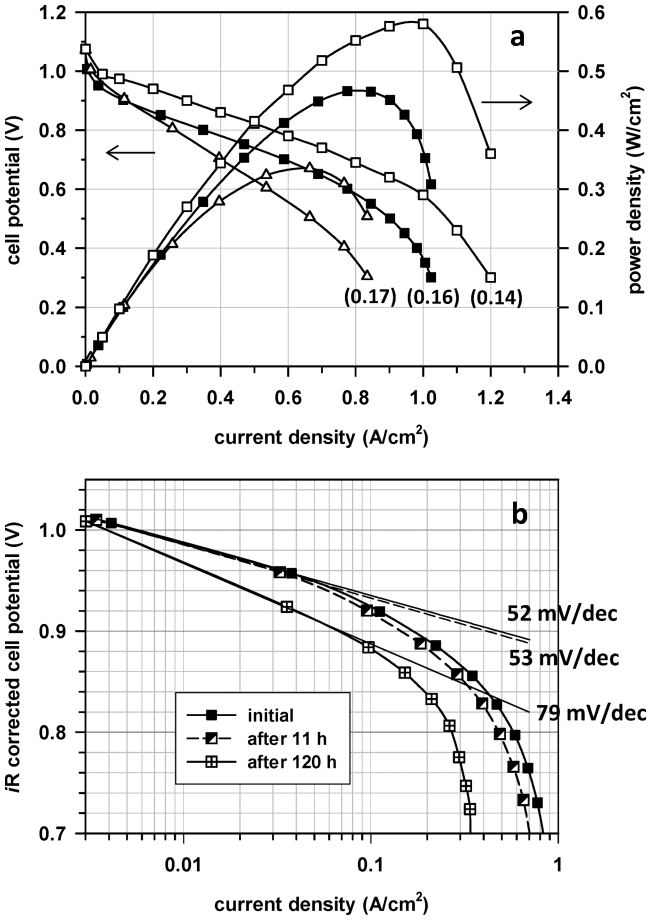

Figure 8. (a) AMFC performance comparison of MEAs using M-Nafion-FA-TMG (■, □) and using ATM-PP (Δ) ionomers at 80 °C; filled symbol: H_2/air (CO_2 = 10 ppm) conditions, unfilled symbol: H_2/O_2 conditions; In both cases, same ATM-PP membranes (thickness = 50 μm) were used; numbers in parentheses are HFR in Ω cm². (b) *iR* corrected cell polarization curves of the MEA using M-Nafion-FA-TMG after extended-term AMFC operation under 80 °C H_2/air conditions.

higher temperature is promising and qualitatively agree well with the *ex situ* testing result (Figure 6). It is believed that the *Tafel-slope* change over time is partly due to the hydrolysis of amide group of the ionomer. Developing strategies to prevent the hydrolysis and optimizing electrode structure may warrant further improved AMFC performance and durability.

4. CONCLUSIONS

Sulfone−pentamethylguanidinium and phenylpentamethylguanidinium functionalized perfluorinated ionomers were successfully synthesized via activated fluoroamine reaction and followed by methylation reaction with DMS for catalyst binders of AMFC applications. While the sulfone guanidinium ionomer exhibited a fast degradation within 24 h with 0.5 M NaOH treatment at 80 °C, the phenylguanidinium ionomer has excellent cation stability after 72 h under the same conditions. Spectroscopic results indicated a nonconjugated structure for sulfone guanidinium and a resonance stabilized structure for phenylguanidinium. Density functional theory calculation showed that the hydrolysis of sulfone−pentamethylguanidinium occurs in a barrierless manner while the barrier energy for the phenylpentamethylguanidinium is 23.8 kcal/mol. AMFC performance using the phenylguanidinium ionomer in the catalyst layers obtained under H_2/O_2 and H_2/air operating conditions was substantially better than those using poly-aromatic ionomers, suggesting that the guanidinium functionalized perfluorinated ionomer rendered desirable electrode structure for the electrochemical reactions in AMFC. The perfluorinated ionomer showed promising stability during 120 h H_2/air AMFC operation. We envisage that such perfluorinated ionomers may be especially useful in cases when reactant gas transport limits the AMFC performance in the presence of liquid water.

■ ASSOCIATED CONTENT

Ⓢ Supporting Information

FT-IR spectrum of 1,1,3,3-tetramethylguanidinium, ^{1}H NMR of M-Nafion-FA-TMG and ^{13}C NMR spectra of M-Nafion-TMG, and a barrier energy comparison. This material is available free of charge via the Internet at http://pubs.acs.org/

■ AUTHOR INFORMATION

Corresponding Author

* E-mail: (Y.S.K.) yskim@lanl.gov.

Present Address

#Lotte Chemical, Daejeon, South Korea.

Notes

The authors declare no competing financial interest.

■ ACKNOWLEDGMENTS

This work was supported by the US Department of Energy at Los Alamos National Laboratory operated by Los Alamos National Security LLC under Contract DE-AC52-06NA25396. Sandia National Laboratory is a multiprogram laboratory operated by Sandia Corporation, a wholly owned subsidiary of Lockheed Martin Company, for the U.S. Department of Energy's National Nuclear Security Administration under Contract DE-AC04-94AL85000. The authors also thank US DOE Fuel Cell Technologies Program, Technology Development Manager Dr. Nancy Garland, for financial support. Y.-K.C acknowledges financial support from the Ministry of Economy, Trade and Industry of Japan through Japan−US cooperation on clean energy technology program.

■ REFERENCES

(1) (a) Perry, M. L.; Fuller, T. F. *J. Electrochem. Soc.* **2002**, *149*, S59−S67. (b) Raistrick, I. D. In *Diaphragms, Separators, and Ion Exchange Membranes*, Van Zee, J. W., White, R. E., Kinoshita, K., Burney, H. S., Eds.; The Electrochemical Society: Pennington, NJ, 1986; p 172.

(2) (a) Wilson, M. S.; Gottesfeld, S. *J. Electrochem. Soc.* **1992**, *139*, L28−L30. (b) Wilson, M. S.; Gottesfeld, S. *J. Appl. Electrochem.* **1992**, *22*, 1−7.

(3) (a) Meng, H.; Shen, P. K. *Electrochem. Commun.* **2006**, *8*, 588−594. (b) Gong, K. P.; Du, F.; Xia, Z. H.; Durstock, M.; Dai, L. M. *Science* **2009**, *323*, 760−764. (c) Li, Y.; Zhou, W.; Wang, H.; Xie, L.; Liang, Y.; Wei, F.; Idrobo, J.-C.; Pennycook, S. J.; Dai, H. *Nature Nanotechnol.* **2012**, *7*, 394−400.

(4) (a) Varcoe, J. R.; Slade, R. C. T.; Yee, E. L. H. *Chem. Commun.* **2006**, *13*, 1428−1429. (b) Varcoe, J. R.; Slade, R. C. T.; Yee, E. L. H.; Poynton, S. D.; Driscoll, D. J.; Apperley, D. C. *Chem. Mater.* **2007**, *19*, 2686−2693. (c) Pan, J.; Lu, S. F.; Li, Y.; Huang, A. B.; Zhuang, L.; Lu, J. T. *Adv. Funct. Mater.* **2010**, *20*, 312−319. (d) Steinbach, A. Presented at the US DOE 2013 Annual Merit Review and Peer Evaluation Meeting, May 13−17, 2013, Washington, DC, 2013. (e) Piana, M.; Boccia, M.; Filpi, A.; Flammia, E.; Miller, H. A.; Orsini,

M.; Salusti, F.; Santiccioli, S.; Ciardelli, F.; Pucci, A. *J. Power Sources* **2010**, *195*, 5875−5881.
(5) (a) Easton, E. B.; Astill, T. D.; Holdcroft, S. *J. Electrochem. Soc.* **2005**, *152*, A752−A758. (b) Ramani, V.; Swier, S.; Shaw, M. T.; Weiss, R. A.; Kunz, H. R.; Fenton, J. M. *J. Electrochem. Soc.* **2008**, *155*, B532−B537. (c) Nakajima, T.; Tamaki, T.; Ohashi, H.; Yamaguchi, T. *J. Phys. Chem. C* **2012**, *116*, 1422−1428.
(6) (a) Ugo, P.; Bertoncello, P.; Vezza, F. *Electrochim. Acta* **2004**, *49*, 3785−3793. (b) Matsui, K.; Kikuchi, Y.; Hiyama, T.; Tobita, E.; Kondo, K.; Akimoto, A.; Seita, T.; Watanabe, H.; US Patent 4,659,744, 1987.
(7) (a) Matsui, K.; Tobita, E.; Sugimoto, K.; Kondo, K.; Seita, T.; Akimoto, A. *J. Appl. Polym. Sci.* **1986**, *32*, 4137−4143. (b) Kong, X.; Wadhwa, K.; Verkade, J. G.; Schmidt-Rohr, K. *Macromolecules* **2009**, *42*, 1659−1664. (c) Jung, M. S. J.; Arges, C. G.; Ramani, V. *J. Mater. Chem.* **2011**, *21*, 6158−6160. (d) Salerno, H. L. S.; Beyer, F. L.; Elabd, Y. A. *J. Polym. Sci., Part B: Polym. Phys.* **2012**, *50*, 552−562. (e) Salerno, H. L. S.; Elabd, Y. A. *J. Appl. Polym. Sci.* **2013**, *1*, 298−307.
(8) (a) Unlu, M.; Abbott, D.; Pamaswamy, N.; Ren, X.; Mukerjee, S.; Kohl, P. A. *J. Electrochem. Soc.* **2011**, *158*, B1423−B1431. (b) Kim, Y. S. Presented at the U.S. DOE Hydrogen Program and Vehicle Technologies Program Annual Merit Review and Peer Evaluation Meeting, May 9−13, 2011, Washington, DC, 2011. (c) Konopka, D.; Johnson, M. A.; Errico, M.; Bahrami, P.; Hays, C. C. *Electrochem. Solid State Lett.* **2012**, *15*, B17−B19. (d) Kim, Y. S.; Fujimoto, C.; Hibbs, M.; Choe, Y.-K.; Kim, D.-S.; Chung, H.; Yim, S.-D. Presented at the 224th ECS Meeting, Oct. 27−Nov. 1, 2013, San Francisco, CA, 2013.
(9) (a) Wang, J.; Li, S.; Zhang, S. *Macromolecules* **2010**, *43*, 3890−3896. (b) Lin, X.; Wu, Liang; Liu, Yanbo; Ong, A. L.; Poynton, S. D.; Varcoe, J. R.; Xu, T. *J. Power Sources* **2012**, *217*, 373−380.
(10) (a) Zhang, W.; Li, S.; Zhang, S. *Chem. Commun.* **2010**, *46*, 7495−7497. (b) Qu, C.; Zhang, H. M.; Zhang, F. X.; Liu, B. *J. Mater. Chem.* **2012**, *22*, 8230−8207.
(11) (a) Kim, D. S.; Kim, Y. S. *ECS Trans.* **2010**, *33*, 1867−1874. (b) Kim, D. S.; Labouriau, A.; Guiver, M. D.; Kim, Y. S. *Chem. Mater.* **2011**, *23*, 3795−3797.
(12) Frisch, M. J.; Trucks, G. W.; Schlegel, H. B.; Scuseria, G. E.; Robb, M. A.; Cheeseman, J. R.; Scalmani, G.; Barone, V.; Mennucci, B.; Petersson, G. A.; Nakatsuji, H.; Caricato, M.; Li, X.; Hratchian, H. P.; Izmaylov, A. F.; Bloino, J.; Zheng, G.; Sonnenberg, J. L.; Hada, M.; Ehara, M.; Toyota, K.; Fukuda, R.; Hasegawa, J.; Ishida, M.; Nakajima, T.; Honda, Y.; Kitao, O.; Nakai, H.; Vreven, T.; Montgomery, J. A., Jr.; Peralta, J. E.; Ogliaro, F.; Bearpark, M.; Heyd, J. J.; Brothers, E.; Kudin, K. N.; Staroverov, V. N.; Kobayashi, R.; Normand, J.; Raghavachari, K.; Rendell, A.; Burant, J. C.; Iyengar, S. S.; Tomasi, J.; Cossi, M.; Rega, N.; Millam, J. M.; Klene, M.; Knox, J. E.; Cross, J. B.; Bakken, V.; Adamo, C.; Jaramillo, J.; Gomperts, R.; Stratmann, R. E.; Yazyev, O.; Austin, A. J.; Cammi, R.; Pomelli, C.; Ochterski, J. W.; Martin, R. L.; Morokuma, K.; Zakrzewski, V. G.; Voth, G. A.; Salvador, P.; Dannenberg, J. J.; Dapprich, S.; Daniels, A. D.; Farkas, Ö.; Foresman, J. B.; Ortiz, J. V.; Cioslowski, J.; Fox, D. J. *Gaussian 09*, revision A.1; Gaussian, Inc.: Wallingford, CT, 2009.
(13) Chai, J.-D.; Head-Gordon, M. *Phys. Chem. Chem. Phys.* **2008**, *10*, 6615−6620.
(14) Hehre, W. J.; Ditchfie, R.; Pople, J. A. *J. Chem. Phys.* **1972**, *56*, 2257−2261.
(15) Tomasi, J.; Mennucci, B.; Cammi, R. *Chem. Rev.* **2005**, *105*, 2999−3093.
(16) (a) Hibbs, M. R.; Fujimoto, C. H.; Cornelius, C. J. *Macromolecules* **2009**, *42*, 8316−8321. (b) Fujimoto, C. H.; Kim, D. S.; Hibbs, M.; Wrobleski, D.; Kim, Y. S. *J. Membr. Sci.* **2012**, *423*, 438−449.
(17) (a) Zingaro, R. A. *J. Am. Chem. Soc.* **1954**, *76*, 814−816. (b) Bellamy, L. J. *The Infrared Spectra of Complex Molecules*: Chapman & Hall: London and New York, 1980. (c) Huczynski, A.; Janczak, J.; Stefanska, J.; Rutkowski, J.; Brzezinski, B. *J. Mol. Struct.* **2010**, *977*, 51−55.
(18) (a) Anderson, M. L.; Hammer, R. N. *J. Chem. Eng. Data* **1967**, *12*, 442−447. (b) Brzezinski, B.; Radziejewski, R.; Zundel, G. *J. Chem. Soc., Faraday Trans.* **1995**, *91*, 3141−3146. (c) Gierczyk, B.; Schroeder, G.; Przybylski, P.; Brzezinski, B. *J. Mol. Struct.* **2006**, *794*, 230−236.
(19) (a) Zhao, G. X.; Chen, B. J.; Qian, S. A. *J. Anal. Appl. Pyrolysis* **1992**, *23*, 87−97. (b) Miyake, M.; Yamada, K.; Oyama, N. *Langmuir* **2008**, *24*, 8527−8532. (c) Pereira, F. S.; DeAzevedo, E. R.; Silva, E. F.; Bonagamba, T. J.; Agostini, D. L. D.; Magalhaes, A.; Job, A. E.; Gonzalez, E. R. P. *Tetrahedron* **2008**, *64*, 10097−10106.
(20) (a) Colthup, N. B.; Daly, L. H.; Wiberley, S. E. *Introduction to Infrared and Raman Spectroscopy*; Academic Press, Inc.: New York, San Francisco, CA, and London, 1975; (b) Schwesinger, R.; Link, R.; Wenzi, P.; Kossek, S.; Keller, M. *Chem.—Eur. J.* **2006**, *12*, 429−437. (c) Thomas, O. D.; Soo, K. J. W. Y.; Peckham, T. J.; Kulkarni, M. P.; Holdcroft, S. *J. Am. Chem. Soc.* **2012**, *134*, 10753−10756. (d) Qu, C.; Zhang, H. M.; Zhang, F. X.; Liu, B. *J. Mater. Chem.* **2012**, *22*, 8203−8207.
(21) Pereira, F. S.; DeAzevedo, E. R.; Silva, E. F.; Bonagamba, T. J.; Agostini, D. L. D.; Magalhaes, A.; Job, A. E.; Gonzalez, E. R. P. *Tetrahedron* **2008**, *64*, 10097−10106.
(22) (a) Kim, Y. S.; Pivovar, B. S. *Annu. Rev. Chem. Biomol. Eng.* **2010**, *1*, 123−148. (b) Kim, Y. S.; Kim, D. S.; Guiver, M. D.; Pivovar, B. S. *J. Membr. Sci.* **2011**, *374*, 49−58.
(23) Choe, Y.-K.; Henson, N.; Kim, Y. S. Presented at the Advances in Materials for Proton Exchange Membrane Fuel Cells Systems, ACS Polymer Division Specialized Workshop, Feb. 17−20, 2013, Asilomar Conference Grounds, Pacific Grove, CA, 2013.
(24) Wang, Y.-J.; Qiao, J.; Baker, R.; Zhang, J. *Chem. Soc. Rev.* **2013**, *42*, 5768−5787.
(25) Pivovar, B. S.; Kim, Y. S. *J. Electrochem. Soc.* **2007**, *154*, B739−B744. (b) Kim, Y. S.; Pivovar, B. S. *J. Electrochem. Soc.* **2010**, *157*, B1602−B1607. (c) Kim, Y. S.; Pivovar, B. S. *J. Electrochem. Soc.* **2010**, *157*, B1616−B1623.